Progress in Neuropsychopharmacology & Biological Psychiatry 111 (2021) 110404

Contents lists available at ScienceDirect

Progress in Neuropsychopharmacology & Biological Psychiatry

journal homepage: www.elsevier.com/locate/pnp

Structural correlates of trauma-induced hyperarousal in mice

Julia Ruat [a,b], Daniel E. Heinz [c,d], Florian P. Binder [b,e], Tibor Stark [f,g], Robert Neuner [c,1], Alice Hartmann [c], Paul M. Kaplick [c], Alon Chen [a,h], Michael Czisch [f], Carsten T. Wotjak [c,d,i,*]

[a] Department Stress Neurobiology and Neurogenetics, Max Planck Institute of Psychiatry, 80804 Munich, Germany
[b] International Max Planck Research School for Translational Psychiatry (IMPRS-TP), 80804 Munich, Germany
[c] Research Group Neuronal Plasticity, Max Planck Institute of Psychiatry, 80804 Munich, Germany
[d] Max Planck School of Cognition, 04103 Leipzig, Germany
[e] Department Translational Research in Psychiatry, Max Planck Institute of Psychiatry, 80804 Munich, Germany
[f] Scientific Core Unit Neuroimaging, Max Planck Institute of Psychiatry, 80804 Munich, Germany
[g] Department of Pharmacology, Faculty of Medicine, Masaryk University, 62500 Brno, Czechia
[h] Department of Neurobiology, Weizmann Institute of Science, 76100 Rehovot, Israel
[i] Central Nervous System Diseases Research (CNSDR), Boehringer Ingelheim Pharma GmbH & Co KG, 88397, Biberach an der Riss, Germany

ARTICLE INFO

Keywords:
Post-traumatic stress disorder
Hyperarousal
Magnetic resonance imaging
Grey matter volume
Animal model

ABSTRACT

Post-traumatic stress disorder (PTSD) is a chronic disease caused by traumatic incidents. Numerous studies have revealed grey matter volume differences in affected individuals. The nature of the disease renders it difficult to distinguish between *a priori versus* a posteriori changes. To overcome this difficulty, we studied the consequences of a traumatic event on brain morphology in mice before and 4 weeks after exposure to brief foot shocks (or sham treatment), and correlated morphology with symptoms of hyperarousal. In the latter context, we assessed hyperarousal upon confrontation with acoustic, visual, or composite (acoustic/visual/tactile) threats and integrated the individual readouts into a single Hyperarousal Score using logistic regression analysis. MRI scans with subsequent whole-brain deformation-based morphometry (DBM) analysis revealed a volume decrease of the dorsal hippocampus and an increase of the reticular nucleus in shocked mice when compared to non-shocked controls. Using the Hyperarousal Score as regressor for the post-exposure MRI measurement, we observed negative correlations with several brain structures including the dorsal hippocampus. If the development of changes with respect to the basal MRI was considered, reduction in globus pallidus volume reflected hyperarousal severity. Our findings demonstrate that a brief traumatic incident can cause volume changes in defined brain structures and suggest the globus pallidus as an important hub for the control of fear responses to threatening stimuli of different sensory modalities.

1. Introduction

Post-traumatic stress disorder (PTSD) is a severe psychiatric disease that may develop after an exposure to a traumatic event such as combat experience, natural disasters or sexual abuse. It is characterized by intrusive symptoms, avoidance behavior, negative changes in thought, and hyperarousal, with these symptoms persisting for longer than a month (Del Barrio, 2016). During the last decades, numerous studies aimed at examining molecular and brain morphological changes occurring in the aftermath of the traumatic incident. Key brain areas of interest became the hippocampus, the prefrontal cortex, and the amygdala (Armony et al., 2005; Gilbertson et al., 2002; O'Doherty et al., 2015; Shin et al., 2004; Wignall et al., 2004; Woodward et al., 2006; Yamasue et al., 2003). Neuroimaging methods, such as magnetic resonance imaging (MRI), allow to assess brain volumetric changes of patients diagnosed with PTSD. However, human studies come with the limitations of heterogenous samples (*e.g.*, severity of the trauma or medical treatment) and methodology, often leading to controversial results. While a number of studies found no volumetric changes in the hippocampus of patients with PTSD (Bonne et al., 2001; Carrion et al., 2001; De Bellis et al., 2001; Fennema-Notestine et al., 2002), others reported reduced hippocampal volume compared to controls (Gilbertson et al., 2002; Logue et al., 2018; Wignall et al., 2004). Noteworthy, such studies rarely involved longitudinal designs with measurements before

* Corresponding author at: Research Group Neuronal Plasticity, Max Planck Institute of Psychiatry, Kraepelinstrasse 2-10, 80804 Munich, Germany.
E-mail address: wotjak@psych.mpg.de (C.T. Wotjak).
[1] deceased.

https://doi.org/10.1016/j.pnpbp.2021.110404
Received 4 May 2021; Received in revised form 23 June 2021; Accepted 17 July 2021
Available online 22 July 2021
0278-5846/

and after the trauma. This gains particular importance if one considers that a priori differences in brain volume may serve as susceptibility/resilience factors for the development of PTSD (Gilbertson et al., 2002) and not necessarily consequences of the trauma. Therefore, the monitoring of intraindividual trajectories of brain volume appears to be the most sensitive measure of PTSD-related changes in grey matter volume. To overcome these limitations, several rodent models of PTSD have been established (for reviews see Deslauriers et al., 2018; Verbitsky et al., 2020). We have previously studied consequences of a traumatic experience (*i.e.*, exposure to an electric foot shock (Siegmund and Wotjak, 2007)) on hippocampal volume of inbred mice using *in vivo* and *ex vivo* approaches after long-term incubation of the trauma (Golub et al., 2011). We observed a reduced hippocampal volume (Golub et al., 2011), which coincided with a reduction in synaptic markers at late time points after the trauma (Herrmann et al., 2012). The present study should extend those observations to within-subject measurements before and after the trauma. Moreover, we employed voxel-based whole brain analyses rather than region of interest measurements. In a two-step process, we initially assessed the behavioral consequences of exposure to an inescapable electric foot shock after trauma incubation, with particular focus on the hyperarousal domain. Classically, hyperarousal is measured as a startle response to a sudden loud noise. It is unclear to which extent hyperarousal can be seen in response to stimuli of different sensory modality, such as visual or tactile threats. Based on the various behavioral data, we performed a logistic regression analysis to obtain individual "Hyperarousal Scores" that allowed us to distinguish trauma-exposed animals and controls. In a second step, we conducted longitudinal measurements of brain morphometry using whole-brain MRI scans in new cohorts of mice. Animals were subjected to a basal MRI prior to the foot shock. After trauma incubation, the animals underwent a second MRI scan and subsequent behavioral screening. This experimental design permitted both cross-sectional and longitudinal within-subject analyses. In addition, we could use the individual Hyperarousal Scores as regressors to identify brain structures which reflect changes in hyperarousal in a parametric rather than categorical manner.

2. Materials & methods

2.1. Animals

Adult male C57BL/6NRjMpi mice (B6NR, originating from Janvier; $n = 67$, 2–5 months age) were bred in the vivarium of the Max Planck Institute of Biochemistry (Martinsried, Germany). Due to changes in the animal facility of the Max Planck Institute of Psychiatry, the two cohorts of mice had to be housed under different conditions. Animals of the first cohort were group-housed under standard housing conditions in Makrolon type II cages with food and water *ad libitum* and maintained in a 12/12-h inverse light/dark cycle (lights off at 6 am). Behavioral testing took place during the active phase of the mice (between 7 am and 5 pm), except for the trauma protocol which was performed during the light phase. The second cohort of mice was group-housed in Green Line IVC mouse cages with food and water *ad libitum* and maintained in a 12/12-h normal light/dark cycle (lights on at 6 am). Behavioral testing took place during the light phase (between 7 am and 5 pm). After admission at the Max Planck Institute of Psychiatry, mice were permitted a recovery period of at least 10 days before starting with the experiments. Experimental procedures were approved by the Government of Upper Bavaria (Regierung von Oberbayern, 55.2-2532.Vet_02-17-206) and performed according to the European Community Council Directive 2010/63/EEC. All efforts were made to reduce the number of experimental subjects and to minimize, if not exclude, any suffering.

2.2. Behavioral procedures

2.2.1. Trauma protocol

Foot shock delivery and assessment of sensitized and conditioned fear has been performed as previously described (Siegmund and Wotjak, 2007). In brief: On day 0, mice were placed onto a metal grid in a conditioning chamber (cubic shaped) that had been cleaned with alcohol-based disinfectant (Pursept A, Schülke & Mayr GmbH, Norderstedt, Germany). After 198 s, they received two electric foot shocks of 1.5 mA (duration: 2 s), interspaced by 60 s. They were returned to their home cage another 60 s later. Animals of the control group underwent the same procedure without receiving a foot shock. To assess trauma-related sensitized fear, all animals were placed into a neutral test context (cylindric Plexiglas wall, no metal grid but bedding, supplemented with 1% acetic acid) for 3 min 23–35 days after foot shock delivery. On the following day, conditioned fear was tested by re-exposing the mice for 3 min to the conditioning context (chamber, cleaned with Pursept A). The sessions were video-recorded, and the following behavioral measures were scored by an experienced observer unaware of the group affiliations: Freezing time, number of rearings and stretch-attend postures (SAPs).

2.3. Acoustic Startle Response (ASR)

Stimulus-response curves were performed using the SR-LAB Startle Response System (San Diego Instruments, San Diego, USA) with a custom-built animal enclosure. The enclosure consisted of black plastic walls (H17 cm) sitting on the upward bended edges of a plastic floor (L5 x W9 cm). During testing, the enclosure was covered with a lid to prevent the mice from escaping. Movement was detected by a piezo element mounted under the floor of the enclosure and connected to the control unit of the SR-LAB system. The enclosure was placed into a cabinet with the fan turned on. The intensity-response curve protocol consisted of a 5-min habituation period followed by 20 ms white noise pulses of 70 dB (A), 90 dB(A), and 105 dB(A). The pulses were each presented 30 times in a pseudo-randomized order, interspersed with 18 control trials (background noise only, 55 dB(A)). Inter-trial intervals were 13–25 s in length. The startle amplitude was defined as the peak voltage output within the first 100 ms after stimulus onset. The enclosure was cleaned with soap and water after each trial.

2.3.1. Beetle Mania Task (BMT)

The Beetle Mania Task (BMT) was used to study defensive reactions to a combined visual, acoustic, and tactile threat as previously described (Heinz et al., 2017). In brief: Experiments were performed in an arena (L150 × W15 × H37 cm for Experiment 1 and L100 × W15 × H37 for Experiment 2) made of grey polyethylene under low light conditions (<50 lx). During the initial habituation phase of 5 min, mice were inserted to one end of the arena, and the latency to reach the opposite end segment as well as the number of rearings were scored. In the end of the habituation phase, we inserted an erratically moving robo-beetle (Hexbug Nano, Innovation First Labs Inc., Greenville, TX, USA) far most distant from the mouse and scored the following behavioral measures over the course of 10 min: (1) contacts (number of physical contacts between the beetle and the mouse), (2) passive behavior (tolerance of the approaching or by-passing beetle), (3) avoidance behavior (whereby the mouse withdrew from the robo-beetle with accelerated speed), (4) approach behavior (events during which the mouse followed the by-passing robo-beetle in close vicinity), and (5) jumps. The behavioral measures (2)–(5) were expressed as the percentage of the number of contacts.

2.3.2. Visual Threat Task (VTT)

This task exposed the animals to two visual threats: a sweeping dot (SD) (De Franceschi et al., 2016), followed by a looming disk (LD) (Yilmaz and Meister, 2013). The visual stimuli were presented in a white Plexiglas arena (L34 x W47 x H30 cm; 70 lx in the center) equipped with an opaque triangular shelter (W19 x H11.5 cm; 10 lx) in the corner (De Franceschi et al., 2016). A monitor (L30 x W47.5 cm, Samsung SyncMaster T220, 60 Hz) was placed on top of the arena, leaving a gap for the camera (DMK 23UV024, The Imaging Source) to capture the mouse

movements. The SD stimulus was a black dot of 3 cm diameter presented in one corner of the display. The dot moved diagonally over the screen four times with a speed of 0.1 m/s. The LD stimulus was a black dot of 3 cm diameter presented in the center of the screen, that expanded in size to 21 cm diameter within 250 ms. The stimulus was repeated 20 times. Both stimuli had a total duration of 20 s and were presented on a grey background. The VTT was performed on two consecutive days. On the first day, the animals were habituated to the arena for 15 min without behavioral analysis. During this time, the arena was covered with the monitor presenting the grey screen without any stimulus. On the next day, animals were habituated to the arena for another 5 min (baseline), with presentation of the grey screen. Thereafter, the sweeping stimulus was triggered, and the behavior was recorded for 5 min after stimulus onset. In the third phase, the looming disk stimulus was presented, and the behavior was monitored for another 5 min. The stimuli were only triggered once the animals were located in the center of the arena. The test was stopped, and the behavior not further analyzed, if an animal failed to leave the shelter for 30 min. Therefore, the total test time could differ significantly between the animals. We considered the following behavioral measures: Number of rearings, freezing duration, the time spent in the shelter, and the latency to enter the shelter after the onset of the stimulus (if a mouse did not enter the shelter within the 20 s after stimulus onset, we assigned an escape latency of 21 s).

2.3.3. *In vivo magnetic resonance imaging (MRI) and deformation-based morphometry (DBM) analysis*

Anesthesia was initiated and maintained using isoflurane (cp-pharma, Burgdorf, Germany). Mice were then stereotactically fixed on an MR compatible animal bed in prone position. Eye ointment (Bepanthen, BAYER AG, Leverkusen, Germany) was applied to protect the eyes from dehydration. Respiration and body temperature were constantly monitored. Body temperature was kept between 36.5 °C and 37.5 °C, using a water flow heating pad (Haake S 5P, Thermo Fisher Scientific, Waltham, United States).

MRI experiments were run on a BioSpec 94/20 animal MRI system operating on Paravision 6.0.1 (Bruker BioSpin GmbH Rheinstetten, Germany) equipped with a 9.4 T horizontal bore magnet of 20 cm diameter and a two-channel cryogenic transmit-receive radio frequency coil. Structural images were recorded using a 3D gradient echo sequence with a repetition time of 34.1 ms, echo time = 6.25 ms, excitation pulse angle = 10°, number of averages = 3, matrix dimension = 256 × 166 × 205, pixel resolution 77 μm. After visual inspection of the data and exclusion of certain mice due to motion artefacts, a total of 20 animals were included in the final analysis.

Images were converted to NIFTI format, with the voxel size of mice image data artificially multiplied by ten (in order to fully exploit analysis pipelines optimized for the human sized brain).

In a two-step procedure, brain extraction was performed: In a first preprocessing step, mouse data was segmented and bias corrected using Statistical Parametric Mapping software (SPM12, Wellcome Department of Cognitive Neurology, London, UK) and the Hikishima C57Bl6 template (Hikishima et al., 2017) comprised of 5 different compartments. The resulting bias-corrected images were filtered using a spatial adaptive non-local means denoising filter (Manjón et al., 2010) as implemented in the cat12 toolbox of SPM (www.neuro.uni-jena.de/cat). The initial grey matter (GM), white matter (WM) and cerebrospinal fluid (CSF) probability maps were summed, and binarized for image intensities larger 0.3, to create a first brain mask. Holes in this mask were filled using MATLAB's (MathWorks, Natick, Massachusetts, USA) imfill function, the mask was dilated by five voxels, and applied to the bias-corrected spatially filtered images. In a second step, the resulting images were again segmented, this time using a modified version of the Hikishima template for which the original CSF template was divided into two sub-templates: ventricular inner CSF and surface cortical CSF. After this second segmentation step, GM, WM and ventricular inner CSF compartments were again summed, binarized using an intensity threshold >0.1, and remaining holes inside the brain mask filled and slightly dilated. Finally, the resulting mask was applied to the spatially filtered and bias corrected images of the first step. These brain-extracted 3D images were then segmented using the SPM12 old segment function, now using only three compartments of the modified version of the Hikishima template, namely GM, WM and inner ventricular CSF.

For cross-sectional DBM analyses focusing on the second experimental time point, DARTEL normalization first imported the brain extracted images of two segments (GM, WM), and a study-specific template based on GM and WM was generated in seven iterations, along with flow-fields which parameterize the deformations. The flow-fields were then converted to Jacobian determinant fields, which were spatially smoothed with a Gaussian kernel of about 6 times the voxel size.

Longitudinal analysis used the rodent longitudinal toolbox (RLT, Version 1; dbm.neuro.uni-jena.de) for SPM12. Bias corrected images (no brain extraction) entered the RLT analysis. Again, C57Bl6 Hikishima templates were used, with a maturation rate of 45 (adult mice). The Jacobian determinant fields for each set of measurements were calculated with respect to the subject's temporal average image, and then subtracted from each other to generate a deformation image from MRI 1 to 2 (Jacobian difference images). The average images per subject were used to create a DARTEL study specific template. Finally, the Jacobian difference images were normalized to the template space and smoothed with a Gaussian kernel of about 6 times the voxel size.

Total intracranial volume (TIV) was approximated as the sum of all modulated tissue probabilities (for the longitudinal analysis, these were derived from the temporal average images), excluding the olfactory bulb and the cerebellum, as well as brain regions inferior to the anterior commissure, due to lower signal-to-noise in these regions because of the surface coil characteristics.

2.4. *Experiments*

In a first step, we assessed behavioral changes of mice in response to a traumatic event and described these in a Hyperarousal Score (Experiment 1). Subsequently, we applied the same mathematical approach to a new batch of mice, which were repeatedly scanned in the MRI before behavioral screening (Experiment 2) in order to relate volumetric changes of the brain to individual behavioral consequence of the trauma.

2.4.1. *Experiment 1: long-term consequences of a traumatic experience*

To examine long-term effects of a traumatic event on defensive responses to threatening stimuli of different sensory modality, we randomly assigned B6NR mice to two groups which either received two electric foot shocks (S+, $n = 24$) or not (S-, $n = 20$). Three weeks later, we measured generalized fear upon exposure to the neutral context (cylinder), followed by measurement of conditioned fear upon re-exposure to the shock context (chamber) 24 h later. Subsequently, all mice underwent the ASR, the VTT and the BMT, with one week of recovery in between two tests.

2.4.2. *Experiment 2: structural correlates of defensive reactions*

Experimentally naïve B6NR mice underwent a first MRI scan (MRI1). After a recovery phase of at least 3 days, we randomly assigned the animals to two groups which either received a foot shock (S+, $n = 11$) or not (S-, $n = 12$), followed by a second MRI scan for both groups (MRI2; 28–30 days later). Thereafter, we assessed generalized and conditioned fear (35 days after foot shock), defensive responses to the robo-beetle (BMT; 41 days after foot shock), acoustic threats (ASR; 47 days after foot shock), and visual threats (VTT; 53 days after foot shock) similarly to Experiment 1.

2.5. *Statistics*

Behavioral data is presented as means ± standard error (SEM), if appropriate. In case of normal distribution, groups were compared by

paired and unpaired *t*-tests, one-way analysis of variance (ANOVA) followed by Tukey's post-hoc test or 2-way analysis of variance (ANOVA) for repeated measures followed by Bonferroni post-hoc analysis. In case of non-parametric distribution, we employed Mann-Whitney *U* tests, and for contingency analyses Chi square tests. Statistically significant differences were accepted if $p < 0.05$. All statistical analyses were performed using GraphPad Prism 8.2.

2.5.1. Logistic regression analysis

We performed a logistic regression analysis in MATLAB R2020a on the z-scores of all readouts of the ASR, BMT, and VTT to predict whether an animal has undergone the preceding PTSD procedure. The analysis was based on the data of Experiment 1. The resulting coefficients were used to calculate the behavior-based Hyperarousal Scores for all animals of both experiments. Therefore, the data of Experiment 2 served as a hold-out validation sample.

2.5.2. MRI

To test the volumetric difference between the shocked and the non-shocked group (MRI2), analysis was run as a two-sample t-test, applying proportional scaling on the TIV to consider unspecific global effects. To test if local brain volumes at MRI2 correlated with the results of the logistic regression on the behavioral readouts, a multiple regression design was used in SPM12, with the TIV entered as a nuisance variable (global normalization using ANCOVA). Volumetric changes between MRI 1 and 2 were analyzed using the Jacobian difference images. Again, TIV was included as nuisance regressor. T-maps were thresholded at an uncorrected $p < 0.005$ or $p < 0.001$ with a minimum cluster extent of 20 voxels. Clusters surviving family-wise error correction as a whole are shown at $p_{FWE,cluster} < 0.05$.

3. Results

3.1. Trauma-related changes in threat responding (Experiment 1)

Experimentally naïve B6NR mice were randomly assigned to two experimental groups. Both groups were placed into a shock chamber, with one group receiving two electric foot shocks (S+), while the other remained non-shocked (S-). Starting 3 weeks later, we assessed generalized trauma-associated fear followed by measurements of hyperarousal upon confrontation with threatening stimuli of different sensory modality.

3.1.1. Generalization of trauma-associated fear memories

S+ mice froze significantly more than S- controls ($U = 7, p < 0.0001$, Fig. 1A) upon exposure to a neutral test context 3 weeks after foot shock (S+) or control exposure to the chamber (S-). Moreover, S+ mice reared less ($U = 0$, $p < 0.0001$, Fig. 1B), which also became evident if we considered the number of mice which failed to rear at all (S+: 42%, S-: 0%; $\chi^2 = 10.8$, $p < 0.01$; Fig. 1B). The behavior of S+ mice cannot be explained by a general decrease in locomotor activity due to a trauma-related reduction in exploratory drive, since S+ showed significantly more risk assessment than S- controls ($U = 51, p < 0.0001$; Fig. 1C). This was reflected by the number of mice which displayed SAPs at all (S+:96%, S-: 40%; $\chi^2 = 16.3$, $p < 0.0001$; Fig. 1C). Re-exposure to the original shock context another day later revealed essentially the same findings with significantly higher freezing levels ($U = 2$, $p < 0.0001$, Fig. 1D), reduced rearing ($U = 13, p < 0.0001$, Fig. 1E; with 61% S+, but 0% S- showing no rearing at all, $\chi^2 = 18.1$, $p < 0.0001$; Fig. 1E) and increased risk assessment ($U = 118$, $p < 0.001$; with 52% S+, but only 5% S- showing risk assessment, $\chi^2 = 11.3$, $p < 0.001$, Fig. 1F).

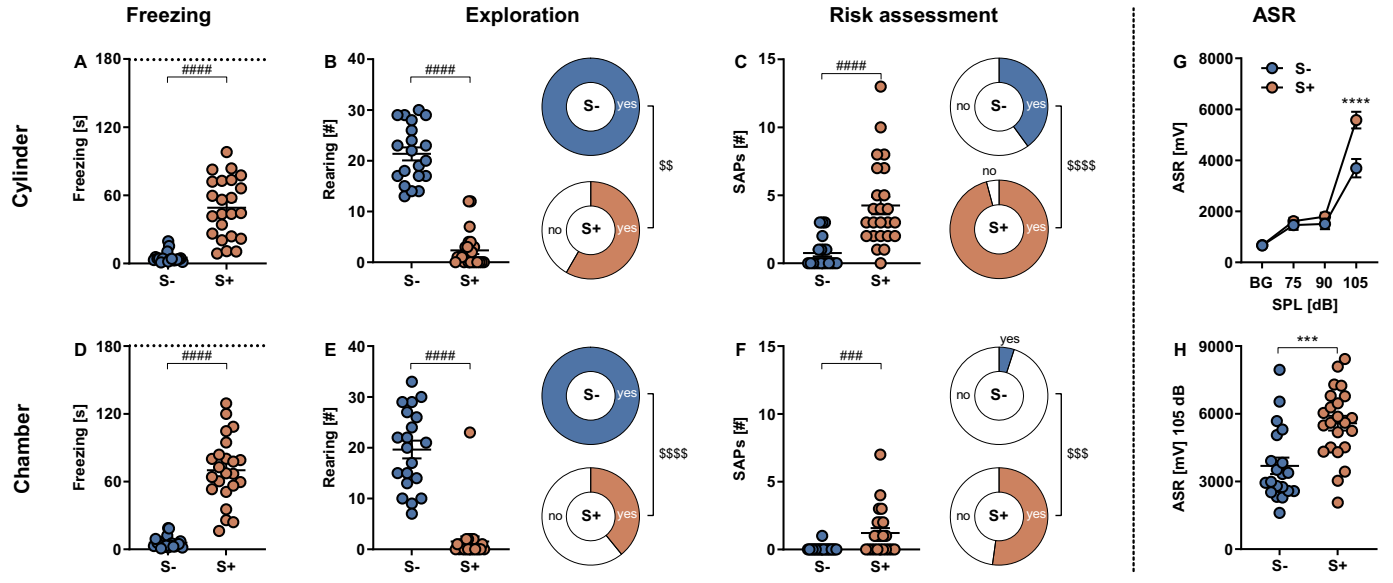

Fig. 1. Generalized trauma-associated fear memory and acoustic startle responses (ASR) after trauma incubation. Mice were (re-)exposed to (A–C) a neutral test context (cylinder) and (D–F) the shock context (chamber) 23 and 24 days after they had received electric foot shocks in the shock chamber (S+) or not (S-). We assessed (A, D) freezing behavior, (B, E) the number of rearings per mouse, as well as the proportion of mice per group which reared at all, and (C, F) risk assessment on basis of the number of stretch-attend postures (SAPs) per mouse and as the proportion of mice which showed SAPs at all. (G) Intensity-response relationship between sound-pressure levels (SPL) of the white noise pulses and the ASR for S+ and S- mice 6 weeks after foot shock or control exposure. (H) Startle responses elicited by white noise pulses of 105 dB(A). $^{###}p < 0.001$, $^{####}p < 0.0001$ (Mann-Whitney test for (A–F)) and $^{\$\$\$}p < 0.001$, $^{\$\$\$\$}p < 0.0001$ (Chi square test). $^{****}p < 0.0001$ (2-Way ANOVA followed by Bonferroni post-hoc test) and $^{***}p < 0.001$ (unpaired *t*-test).

3.1.2. Acoustic startle response after trauma incubation

Four weeks after foot shock application, we exposed the S+ and S- mice to white noise pulses of different intensity and measured their acoustic startle responses. As revealed by 2-way ANOVA, there was a significant interaction between shock and startle pulse intensity ($F_{3,123} = 11.1, p < 0.0001$). Post-hoc analyses confirmed that S+ mice showed a higher startle response at the highest startle pulse intensity (105 dB(A)) compared to S- controls ($t_{41} = 3.9, p < 0.001$; Fig. 1G–H).

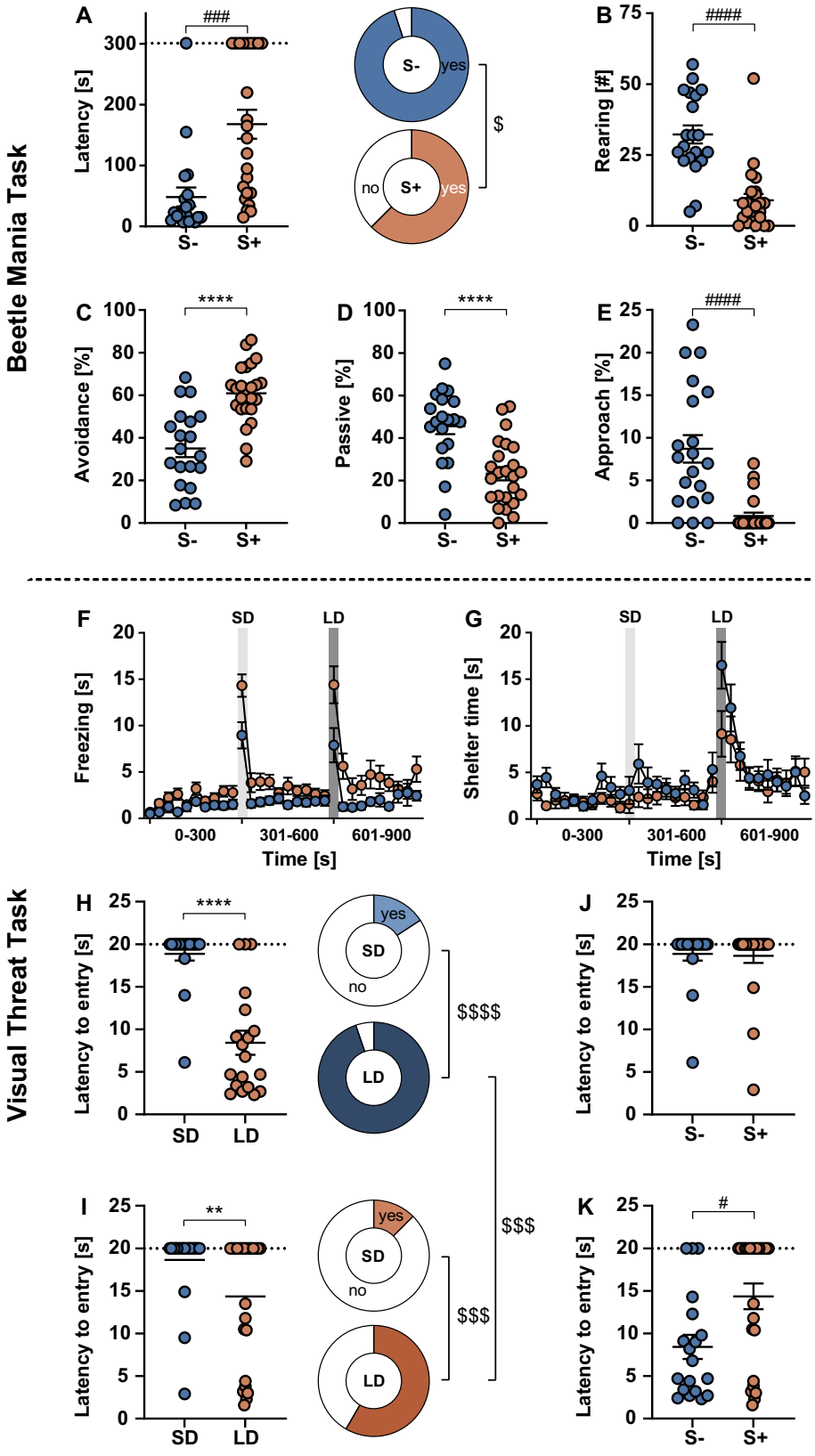

Fig. 2. Beetle Mania Task (A–E) and Visual Threat Task (F–K). In absence of the robo-beetle during the baseline period (0–5 min), we measured (A) horizontal (*i.e.*, latency to end exploration, including information of the proportion of mice which failed to explore the end of the arena at all) and (B) vertical (*i.e.*, number of rearings) exploration in mice with (S+) or without (S-) foot shock administration. (C) Active and (D) passive responses, and (E) approach behavior upon contact with the robo-beetle (expressed as the percentage of the number of contacts) during the subsequent confrontation with a robo-beetle (5–15 min). The time course of freezing responses (F) and the time spent in the shelter (G) during the VTT is presented in 30-s time bins. The time bin of stimulus presentation is highlighted by a grey bar (SD Sweeping Dot, LD Looming Disk). The latency to entering the shelter after stimulus onset (individual data) and the proportions of animals entering the shelter within the 20-s stimulus are presented for S- (H) and the S+ (I) and are directly compared during the SD (J) and LD stimulus (K). $^{\#}p < 0.05$, $^{\#\#\#}p < 0.001$, $^{\#\#\#\#}p < 0.0001$ (Mann Whitney test for (A–B), (F–G) and (K)); $^{****}p < 0.0001$ (unpaired t-test for (D–E)); $^{**}p < 0.01$, $^{****}p < 0.0001$ (paired t-test for (H–I)); $^{\$}p < 0.05$, $^{\$\$}p < 0.01$, $^{\$\$\$}p < 0.001$, $^{\$\$}$ $^{\$\$}p < 0.0001$ (Chi-square test for (A) and (H–I)).

3.1.3. Beetle mania task after trauma incubation

To assess consequences of trauma on active *versus* passive fear responses to a potentially threatening stimulus, we submitted S+ and S- mice to the BMT four weeks after foot shock. During the baseline exploration without robo-beetle (0–5 min), S+ showed significantly reduced horizontal (assessed by the latency to reach the end of the arena; $U = 74$, $p < 0.0001$, Fig. 2A; whereby only 63% compared to 95% of S- reached the opposite end of the arena at all, $\chi^2 = 6.6$, $p < 0.05$; Fig. 2A) and vertical exploration (assessed by the number of rearings; $U = 44.5$, $p < 0.0001$, Fig. 2B).

Subsequent confrontation with the erratically moving robo-beetle (5–15 min) resulted in the same number of contacts (mean S+ = 42.2 ± 1.2 *versus* mean S- = 41.9 ± 1.0, $t_{42} = 0.2$). However, S+ responded differently from S- to the contacts: S+ mice showed an increase in avoidance behavior ($t_{42} = 5.4$, $p < 0.0001$, Fig. 2C) which was mirrored by a corresponding decrease in passive behavior ($t_{42} = 4.6$, $p < 0.0001$, Fig. 2D). Besides, S+ mice reacted with more jumps (range S+ = 0–54, median = 1.5 *versus* range S- = 0–72, median = 8.0, $U = 149.5$, $p < 0.05$) and a lower level of proactive approaching of the bypassing robo-beetle compared to S- controls ($U = 59$, $p < 0.0001$, Fig. 2E).

3.1.4. Visual threat task after trauma incubation

Eight weeks after foot shock, we tested the reaction of S+ and S- mice to two different visual overhead stimuli, following habituation to the setup the day before, and a 5-min basal exposure to the arena on the test day. There were no group differences in freezing (2-way ANOVA RM; $p = 0.51$) and shelter time (2-way ANOVA RM; $p = 0.261$) during baseline (0–300 s). 2-way ANOVA (group, time bin) for repeated measures revealed no differences when comparing the time spent freezing (Fig. 2F) and the time spent in the shelter (Fig. 2G) during the 30-s time bin containing the 20-s SD stimulus presentation (301–330 s) and the following 30-s time bin (331–360 s; statistics not shown). Considering the latency to enter the shelter after the onset of the visual stimulus, both the S- controls ($t_{18} = 7.5$, $p < 0.0001$, (Fig. 2H) and the S+ animals ($t_{23} = 3.0$, $p < 0.01$, Fig. 2I) showed a decreased latency in response to the LD stimulus compared to the SD stimulus. While both groups showed an increase in the number of animals entering the shelter at all in response to the LD compared to the SD stimulus ($\chi^2 = 24.0$, $p < 0.0001$ for S-; $\chi^2 = 11.0$, $p < 0.001$ for S+, Fig. 2H–I), a smaller fraction of S+ animals escaped to the shelter during the LD stimulus compared to S- ($\chi^2 = 13.2$, $p < 0.001$). There was no difference between the groups in the latency to shelter entry during the SD phase ($U = 222$, $p = 0.94$; Fig. 2J), but S+ animals had a higher latency to enter the shelter in response to the LD stimulus ($U = 132.5$, $p < 0.05$, Fig. 2K). In summary, shocked animals tended to express more passive behavior in comparison to non-shocked control animals, irrespective of the nature of the overhead visual stimulus.

3.2. Structural changes in brain morphometry after trauma (Experiment 2).

To assess structural correlates of trauma exposure, an experimentally naïve cohort of B6NR mice underwent a first volumetric MRI scan. Subsequently, the cohort was split into two groups, one receiving two electric foot shocks (S+), while the other remained non-shocked (S-). One month later, both groups were subjected to a second MRI scan. DBM was used to detect morphological differences between the two groups. Whole-brain analysis after the shock (MRI2) revealed a reduced volume of the right dorsal hippocampus, affecting areas CA1 and CA2 (Fig. 3A) and an increased volume of the caudal linear raphe nucleus and the right reticular nucleus (Fig. 3B) in S+ compared to S- mice ($p < 0.005$).

To relate the interindividual variability in PTSD-related symptoms to morphometric measures while reducing the dimensions of the data and, thus, the fallacies associated with multiple comparisons, we decided to condense the different behavioral readouts from ASR, BMT and VVT into a single Hyperarousal Score. We performed a logistic regression analysis based on the z-scores of the individual readouts to predict the condition (S- and S+) of the mice of Experiment 1. The resulting coefficients were used to calculate the Hyperarousal Score for all mice from both experiments (Fig. 4A). In this way, the sample from Experiment 2 served as a hold-out validation sample (data of the individual behavioral tests not shown). The high accuracy of 83% to predict the condition in the hold-out sample supports the stability of the score despite the relatively small sample size in Experiment 2.

The highest positive loadings were dominated by avoidance behavior and latency to explore the arena in the BMT, and the time spent in the shelter during the LD stimulus in the VTT. The strongest negative loadings resulted from rearing behavior in the BMT, time spent in the shelter and latency to enter the shelter during the SD stimulus in the VTT (Table 1).

The inter-individual differences in the individual Hyperarousal Scores of S+ and S- mice from Experiment 2 allowed us to use the behavior-based score as a regressor for volumetric changes. When applied to MRI2, we found that higher Hyperarousal Score values correlated with smaller volumes of the left ventrolateral and lateral orbital cortex, the dorsal and ventral agranular insular cortex, the gustatory cortex (Fig. 4B), the primary somatosensory cortex (Fig. 4B–C), the right ventral part of the caudate putamen (Fig. 4C), the right dorsal hippocampus (specifically the dorsal CA1/CA2/CA3 regions; Fig. 4D) and the right subiculum (Fig. 4E). On the other end, higher Hyperarousal Scores correlated with larger volumes in the right nucleus of the diagonal band (Fig. 4C), the pontine reticular nucleus and the right pontine grey (Fig. 4F; $p < 0.005$; cluster extent >30).

Next, we related the individual Hyperarousal Scores to longitudinal within-subject changes in brain volume from baseline to post-shock conditions (MRI2-MRI1). We obtained a negative correlation between the Hyperarousal Score and the volume change of the right internal and external segment of the globus pallidus (Fig. 4G and H), the secondary motor area, the medial amygdala (Fig. 4H), the dorsal raphe nucleus and

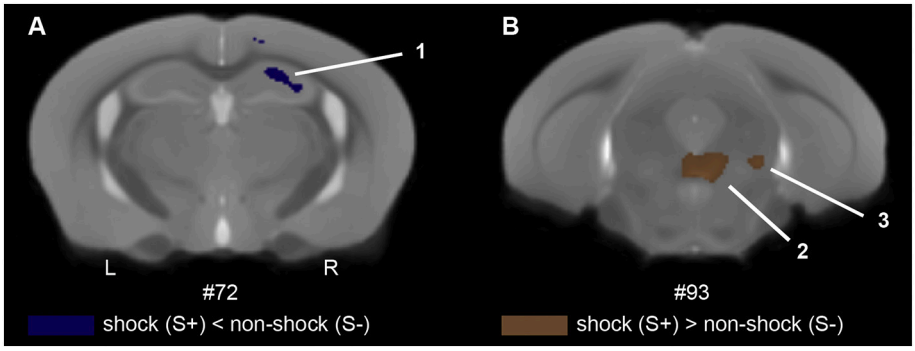

Fig. 3. DBM on brains of trauma-exposed and control mice. Coronal brain slice indicating smaller right dorsal hippocampal volume (A) and an increased volume in the caudal linear raphe nucleus and the right reticular nucleus (B) in S+ mice four weeks after foot shock (MRI2). Brain structures indicated: 1 dorsal hippocampus, 2 caudal linear raphe nucleus, 3 pontine reticular nucleus. Numbers(#) under the slides indicate image numbers of corresponding reference images in the Allen Brain Atlas. Statistical threshold is set at $p < 0.005$, with cluster extent >30.

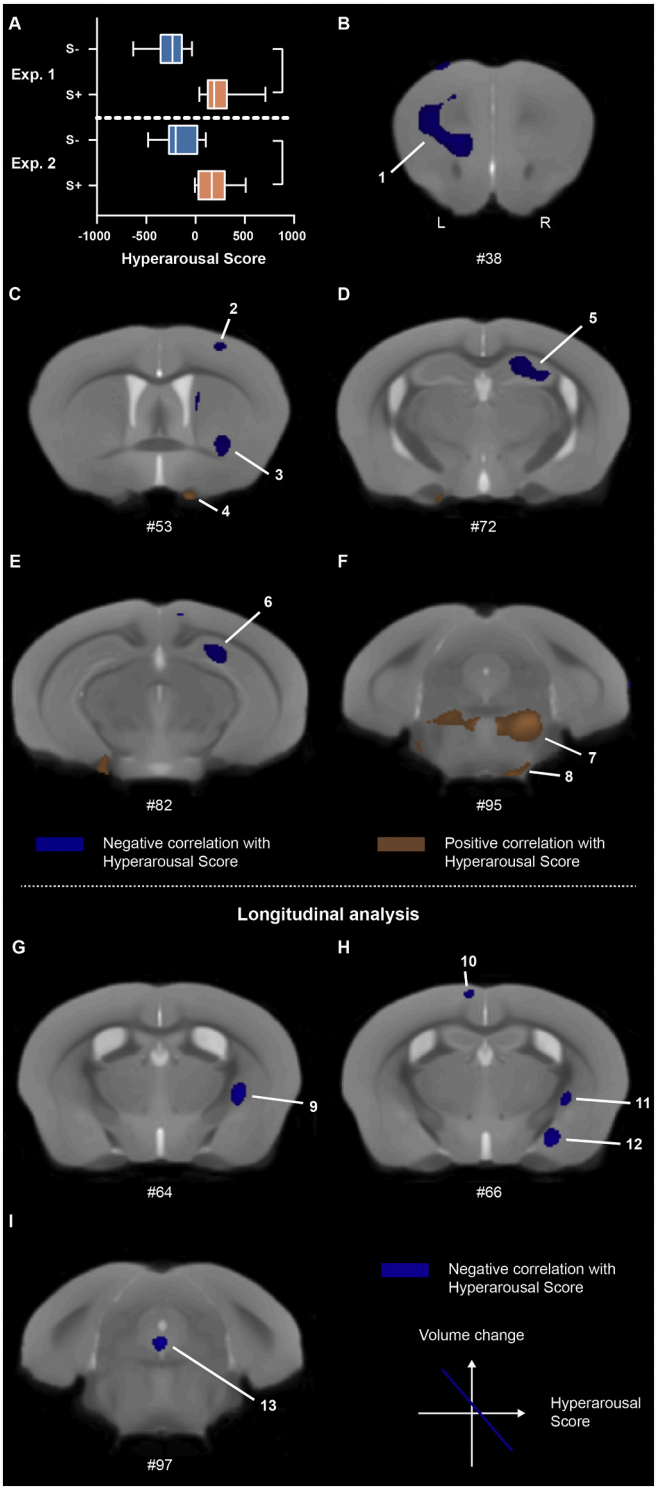

(caption on next column)

Fig. 4. Logistic regression analysis and correlation with brain morphology. Hyperarousal Scores for Experiment 1 and 2 (A). Coronal brain slices indicating brain areas correlating with the Hyperarousal Score at scan time point 2 (B-F; $p < 0.005$, cluster extent >30) and in the longitudinal within-subject analysis (G-I; $p_{FWE,\ cluster} < 0.05$, with a collection threshold of $p < 0.001$). Blue color indicates a negative correlation, brown color indicates a positive correlation with the Hyperarousal Score for (B–I). Brain structures indicated in figures: 1 ventrolateral and lateral orbital cortex, dorsal and ventral agranular insular cortex, gustatory cortex, primary somatosensory cortex; 2 primary somatosensory cortex; 3 ventral caudate putamen; 4 nucleus of the diagonal band; 5 dorsal hippocampus; 6 subiculum; 7 pontine reticular nucleus; 8 pontine grey; 9 + 11 internal and external segment of the globus pallidus; 10 secondary motor area; 12 medial amygdala; 13 dorsal raphe nucleus and the ventromedial periaqueductal grey. Numbers(#) under slides indicate image numbers of corresponding reference images in the Allen Brain Atlas. (For interpretation of the references to color in this figure legend, the reader is referred to the web version of this article.)

the ventromedial periaqueductal grey (Fig. 4I; $p_{FWE,cluster} < 0.05$, with a collection threshold of $p < 0.001$) with higher Hyperarousal Scores correlating with a decrease in volume after trauma incubation.

4. Discussion

We employed a well-established mouse model of PTSD (Siegmund and Wotjak, 2007) to study the association between trauma-related hyperarousal and volumetric changes in the mouse brain. Trauma-exposed mice exhibited increased generalized and conditioned fear reactions, accompanied by increased acoustic startle responses and increased active fear in response to a robo-beetle. The group differences were confirmed by the logistic regression analysis and the resulting Hyperarousal Score. Whole-brain MRI with scans prior to and after trauma exposure allowed for cross-sectional and longitudinal analyses. Shocked animals showed a decreased volume of the dorsal hippocampus and an increase of the reticular nucleus compared to non-shocked controls after trauma. Applying the Hyperarousal Scores as regressor for the cross-sectional analysis after trauma revealed, among others, a negative correlation with the dorsal hippocampus. Further, we found a negative correlation between the regressor and the globus pallidus in the longitudinal within-subject analysis.

PTSD is a disorder defined by symptoms lasting for at least one month. During the last decades, numerous animal models have been established to mimic the disorder in rodents (Verbitsky et al., 2020). Our model (Siegmund and Wotjak, 2007) could show that behavioral changes persist weeks after mice had received electric foot shocks. Besides the classic immobility measures in the conditioning and neutral context, we observed reduced exploratory behavior (rearings) and increased risk assessment (number of SAPs), indicative of increased anxiety-like behavior (Grewal et al., 1997).

Studies showed that combat-exposed PTSD patients exhibit an exaggerated startle response (Orr et al., 1995; Shalev and Rogel-Fuchs, 1992), and hyperarousal is one of the diagnostic criteria for PTSD (Del Barrio, 2016). In our study, we can show that trauma-exposed animals displayed an exaggerated acoustic startle response. Earlier rodent studies, some of them differing in the type of stressor and trauma incubation time, have come to similar results (Bourke and Neigh, 2012; Cohen et al., 2004; Golub et al., 2011; Golub et al., 2009; Pulliam et al., 2010). Aside from classic behavioral tests, we also exposed the mice to more ethobehavioral tasks to test for innate fear responses. Exposure to an erratically moving robo-beetle (Heinz et al., 2017) indicated increased active (*i.e.*, avoidance, jumping) and decreased passive fear responses after trauma incubation. The situation appeared to be different upon confrontation with visual threats, whereby shocked mice showed a trend towards increased freezing not only to the SD (reminiscent of a cruising bird of prey (De Franceschi et al., 2016)) but also in response to a LD (reminiscent of an approaching predator (Yilmaz and Meister, 2013)), when escape would be the appropriate reaction. The lack of statistically significant group differences might be ascribed to the rather long incubation time of more than 8 weeks after foot shock or habituation due to handling associated withthe exposure to previous behavioral tasks.

In order to assess the PTSD-like symptoms not only in a parametric manner but on a continuous scale for symptom intensity, we calculated a Hyperarousal Score based on the individual behavior after trauma incubation. The score does not include measures for generalized fear

Table 1
Behavioral readouts with corresponding loadings of the logistic regression analysis based on Experiment 1 (significant loadings in bold).

Variable	Loading
BMT: Avoidance in response to RB contact	102.51
BMT: Latency to end exploration during baseline	90.02
VTT: Total shelter time during LD	56.51
BMT: Jumps in response to RB contact	30.35
VTT: Total freezing time during SD	26.34
VTT: Freezing time during SD stimulus	25.19
ASR: Startle response at 105 dB(A)	22.78
VTT: Freezing time during first 20 s of baseline	8.94
Intercept	7.54
VTT: Latency to shelter entry in response to LD stimulus	6.15
VTT: Total freezing time during LD	5.98
VTT: Total shelter time during SD	5.40
VTT: Shelter time during first 20 s of baseline	3.43
VTT: Total freezing time during baseline	−12.95
VTT: SAP during SD	−28.96
VTT: Total shelter time during baseline	−31.83
VTT: Shelter time during LD stimulus	−49.75
VTT: Freezing time during LD stimulus	−71.57
VTT: Latency to shelter entry in response to SD stimulus	−75.56
VTT: Shelter time during SD stimulus	−95.88
BMT: Rearing during baseline	−126.11

because of the limited variability of the data and is therefore biased towards the hyperarousal domain. The logistic regression revealed a general increase in hyperarousal and reactivity irrespective of the sensory modalities of the threatening stimuli. This supports a scenario, whereby perception and incubation of the foot shock leads to long-term changes in brain structures generally involved in threat responding, rather than in individual stimulus-response pathways.

To narrow down those brain structures, we combined behavioral assessment with *in vivo* brain volume measurements. We based this attempt on the premise that changes in neuronal activity may result in changes in grey matter volume. Numerous structural MRI studies have been performed comparing PTSD patients and non-traumatized controls or trauma-exposed healthy individuals. Many of them applied region-of-interest-driven approaches and a cross-sectional design. Recent meta-analyses have reported reduced volume of the hippocampus, the amygdala, the anterior cingulate and the occipital cortex in PTSD patients compared to healthy controls without trauma exposure (Bromis et al., 2018; Li et al., 2014; Meng et al., 2014; O'Doherty et al., 2015). The same studies revealed a reduction in the hippocampus, the left temporal gyrus, and the right superior frontal gyrus as well as the left anterior cingulate cortex, and the left insula in PTSD patients compared to trauma-exposed individuals that did not develop PTSD (Li et al., 2014; Logue et al., 2018; Meng et al., 2014; O'Doherty et al., 2015; Woon et al., 2010). In our mouse model we applied a whole brain voxel-wise analysis and could demonstrate a reduction of the right dorsal hippocampus of shocked mice compared to the non-shocked control group. This confirms earlier work from Golub and colleagues applying ultramicroscopy and manganese-enhanced MRI (Golub et al., 2011). Further, we saw a volume increase in the reticular nucleus and the raphe nucleus of trauma-exposed mice, both brain structures being part of the so-called reticular activating system. The reticular nuclei are known to serve a fundamental role in the promotion and maintenance of an arousal state and defensive reactions in rodents and humans (Davis et al., 1982; Steriade, 1996). A recent study found enhanced pedunculopontine nuclei resting state functional connectivity to brain areas involved in threat responding such as the amygdala or the medial prefrontal cortex in individuals with the dissociative subtype PTSD compared to healthy controls (Thome et al., 2019).

Applying the Hyperarousal Score as a regressor for cross-sectional volumetric measures revealed a correlation with two brain structures already identified in the shock/non-shock comparison. We found a negative correlation with the right dorsal hippocampus and a positive correlation with the reticular nucleus. Additionally, the subiculum as part of the hippocampal formation showed a negative correlation with the Hyperarousal Score, indicating a smaller grey matter volume in animals with a high score. Several studies have analyzed volumetric differences in hippocampal subfields in individuals affected with PTSD and controls. Some of these found a reduced volume of the subiculum in PTSD patients (Luo et al., 2017; Teicher et al., 2012) while others failed to reveal differences (Bonne et al., 2008; Chen et al., 2018; Wang et al., 2010). We wish to emphasize that our analysis does not explore categorical differences between trauma-exposed individuals and controls but include the inter-individual differences in the severity of trauma-related hyperarousal regarding brain volume changes (i.e., parametric differences).

Studying PTSD in a mouse model comes with the advantage of standardized trauma intensity and incubation time. But more importantly, it allows us to measure grey matter volume before and after the traumatic event, an experimental design which is difficult to employ in humans. Our longitudinal regression analysis revealed a negative correlation between the Hyperarousal Score and the globus pallidus, the medial amygdala, and the dorsal raphe nucleus/ventral periaqueductal grey area. Animals with a higher severity of symptoms therefore show a volume decrease in these areas. Smaller volumes of the globus pallidus have been linked to higher symptomatic scores in active police soldiers that had been exposed to work-related traumatic events (Shucard et al., 2012). Another study found the globus pallidus as a cluster of decreased neuronal activity in PTSD-affected individuals compared to controls (Disner et al., 2018). However, no volumetric difference in globus pallidus volume was found by Sussmann and colleagues when comparing soldiers with PTSD and combat-exposed controls in a cross-sectional analysis (Sussman et al., 2016).

Several of the volumetric differences were only detected unilaterally in our study. This might be attributed to brain lateralization, a feature conserved across species, including mice (Ehret, 1987; Kawakami et al., 2003). On the other hand, we cannot exclude the possibility that the lack of bilateral evidence is due to the small sample size.

Our study confirms trauma-induced changes in brain morphology as opposed to *a priori* differences which would define individual susceptibility to traumatic events. We can only speculate about the mechanisms underlying the volume changes in response to such events. Previous work has shown that grey matter volume loss can be explained by decreased neurogenesis in dentate gyrus (Gould et al., 1997), loss of dendritic length and branching and reduction in the number of synapses (Kassem et al., 2013; Radley et al., 2006) and decrease in the number of oligodendrocytes (Banasr et al., 2007) in response to stress in rodents. It is conceivable that those structural changes may resemble compensatory mechanisms in neuronal circuits aimed at protecting against devastating consequences of hyperexcitation. Also elevated cortisol levels have been linked to decreases in brain volume, *e.g.*, in the hippocampus (Echouffo-Tcheugui et al., 2018; Fowler et al., 2021; Geerlings et al., 2015; Lupien et al., 1998; Pruessner et al., 2005). In our model, we do not have evidence for sustained changes in corticosterone (Kao et al., 2015), which is different from a subset of patients which even show reduced plasma cortisol levels and increased negative feedback of the HPA axis (Mason et al., 1986; Yehuda et al., 1996). Nevertheless, we cannot rule out that the rise in corticosterone in the early aftermath of the traumatic incident has contributed to the volumetric changes observed several weeks later. It remains to be demonstrated in future studies, to which extent those scenarios account for the trauma-related changes in brain volume observed in the present study.

Our study comes with several limitations, first of which is the relatively small sample size for longitudinal volumetric measures. Due to this power issue, we were only able to characterize the strongest changes. Increasing animal numbers might allow for detecting more subtle structural changes and bilateral effects. This study only includes male mice and the results provided might not be valid when it comes to behavioral and morphological trauma-related changes in females.

Further, our behavioral readouts have a bias towards the hyperarousal domain of PTSD symptoms and do not cover other important symptom criteria such as avoidance of trauma-related cues. The current study provides a correlational analysis which generates hypotheses. It is up to future studies to deliver proofs of functional involvement of the brain areas discussed in the neuronal circuits of PTSD.

5. Conclusion

Our findings demonstrate that a brief traumatic event is sufficient to trigger changes in grey matter volume and that, among others, the globus pallidus plays an important role in the control of fear responses to threats of different sensory modalities.

Ethical statement

Experimental procedures were approved by the Government of Upper Bavaria (Regierung von Oberbayern, 55.2-2532.Vet_02-17-206) and performed according to the European Community Council Directive 2010/63/EEC. All efforts were made to reduce the number of experimental subjects and to minimize, if not exclude, any suffering.

Declaration of Competing Interest

The authors declare no competing interests.

Acknowledgments

This work was supported by the German-Israeli Foundation for Scientific Research and Development (I-1442-421. 13/2017) and by Vienna Science and Technology Fund (CS18-019) to C.T.W.. D.E.H. was supported by the Federal Ministry for Education and Research and the Max Planck Society. A.H. received a fellowship from the Fundação de Amparo à Pesquisa do Estado de São Paulo (BEPE-2018/17387-9). T.S. was supported by the Specific University Research (MUNI/A/1249/2020) provided by MŠMT.

References

Armony, J.L., Corbo, V., Clément, M.H., Brunet, A., 2005. Amygdala response in patients with acute PTSD to masked and unmasked emotional facial expressions. Am. J. Psychiatry 162, 1961–1963. https://doi.org/10.1176/appi.ajp.162.10.1961.

Banasr, M., Valentine, G.W., Li, X.Y., Gourley, S.L., Taylor, J.R., Duman, R.S., 2007. Chronic unpredictable stress decreases cell proliferation in the cerebral cortex of the adult rat. Biol. Psychiatry 62, 496–504. https://doi.org/10.1016/j.biopsych.2007.02.006.

Bonne, O., Brandes, D., Gilboa, A., Gomori, J.M., Shenton, M.E., Pitman, R.K., Shalev, A. Y., 2001. Longitudinal MRI study of hippocampal volume in trauma survivors with PTSD. Am. J. Psychiatry 158, 1248–1251. https://doi.org/10.1176/appi.ajp.158.8.1248.

Bonne, O., Vythilingam, M., Inagaki, M., Wood, S., Neumeister, A., Nugent, A.C., Snow, J., Luckenbaugh, D.A., Bain, E.E., Drevets, W.C., Charney, D.S., 2008. Reduced posterior hippocampal volume in posttraumatic stress disorder. J. Clin. Psychiatry 69, 1087–1091. https://doi.org/10.4088/JCP.v69n0707.

Bourke, C.H., Neigh, G.N., 2012. Exposure to repeated maternal aggression induces depressive-like behavior and increases startle in adult female rats. Behav. Brain Res. 227, 270–275. https://doi.org/10.1016/j.bbr.2011.11.001.

Bromis, K., Calem, M., Reinders, A.A.T.S., Williams, S.C.R., Kempton, M.J., 2018. Meta-analysis of 89 structural MRI studies in posttraumatic stress disorder and comparison with major depressive disorder. Am. J. Psychiatry 175, 989–998. https://doi.org/10.1176/appi.ajp.2018.17111199.

Carrion, V.G., Weems, C.F., Eliez, S., Patwardhan, A., Brown, W., Ray, R.D., Reiss, A.L., 2001. Attenuation of frontal asymmetry in pediatric posttraumatic stress disorder. Biol. Psychiatry 50, 943–951. https://doi.org/10.1016/S0006-3223(01)01218-5.

Chen, L.W., Sun, D., Davis, S.L., Haswell, C.C., Dennis, E.L., Swanson, C.A., Whelan, C.D., Gutman, B., Jahanshad, N., Iglesias, J.E., Thompson, P., Wagner, H.R., Saemann, P., LaBar, K.S., Morey, R.A., 2018. Smaller hippocampal CA1 subfield volume in posttraumatic stress disorder. Depress. Anxiety 35, 1018–1029. https://doi.org/10.1002/da.22833.

Cohen, H., Zohar, J., Matar, M.A., Zeev, K., Loewenthal, U., Richter-Levin, G., 2004. Setting apart the affected: the use of behavioral criteria in animal models of post traumatic stress disorder. Neuropsychopharmacology 29, 1962–1970. https://doi.org/10.1038/sj.npp.1300523.

Davis, M., Parisi, T., Gendelman, D.S., Tischler, M., Kehne, J.H., 1982. Habituation and sensitization of startle reflexes elicited electrically from the brainstem. Science 218, 688–690. https://doi.org/10.1126/science.7134967.

De Bellis, M.D., Hall, J., Boring, A.M., Frustaci, K., Moritz, G., 2001. A pilot longitudinal study of hippocampal volumes in pediatric maltreatment-related posttraumatic stress disorder. Biol. Psychiatry 50, 305–309. https://doi.org/10.1016/S0006-3223(01)01105-2.

De Franceschi, G., Vivattanasarn, T., Saleem, A.B., Solomon, S.G., 2016. Vision guides selection of freeze or flight defense strategies in mice. Curr. Biol. 26, 2150–2154. https://doi.org/10.1016/j.cub.2016.06.006.

Del Barrio, V., 2016. Diagnostic and Statistical Manual of Mental Disorders, 5th Revise. Ed, The Curated Reference Collection in Neuroscience and Biobehavioral Psychology. American Psychiatric Association Publishing, Arlington, USA. https://doi.org/10.1016/B978-0-12-809324-5.05530-9.

Deslauriers, J., Toth, M., Der-Avakian, A., Risbrough, V.B., 2018. Current status of animal models of posttraumatic stress disorder: behavioral and biological phenotypes, and future challenges in improving translation. Biol. Psychiatry 83, 895–907. https://doi.org/10.1016/j.biopsych.2017.11.019.

Disner, S.G., Marquardt, C.A., Mueller, B.A., Burton, P.C., Sponheim, S.R., 2018. Spontaneous neural activity differences in posttraumatic stress disorder: a quantitative resting-state meta-analysis and fMRI validation. Hum. Brain Mapp. 39, 837–850. https://doi.org/10.1002/hbm.23886.

Echouffo-Tcheugui, J.B., Conner, S.C., Himali, J.J., Maillard, P., Decarli, C.S., Beiser, A. S., Vasan, R.S., Seshadri, S., 2018. Circulating cortisol and cognitive and structural brain measures. Neurology 91, E1961–E1970. https://doi.org/10.1212/WNL.0000000000006549.

Ehret, G., 1987. Left hemisphere advantage in the mouse brain for recognizing ultrasonic communication calls. Nature 325, 249–251. https://doi.org/10.1038/325249a0.

Fennema-Notestine, C., Stein, M.B., Kennedy, C.M., Archibald, S.L., Jernigan, T.L., 2002. Brain morphometry in female victims of intimate partner violence with and without posttraumatic stress disorder. Biol. Psychiatry 52, 1089–1101. https://doi.org/10.1016/S0006-3223(02)01413-0.

Fowler, C.H., Bogdan, R., Gaffrey, M.S., 2021. Stress-induced cortisol response is associated with right amygdala volume in early childhood. Neurobiol. Stress 14, 100329. https://doi.org/10.1016/j.ynstr.2021.100329.

Geerlings, M.I., Sigurdsson, S., Eiriksdottir, G., Garcia, M.E., Harris, T.B., Gudnason, V., Launer, L.J., 2015. Salivary cortisol, brain volumes, and cognition in community-dwelling elderly without dementia. Neurology 85, 976–983. https://doi.org/10.1212/WNL.0000000000001931.

Gilbertson, M.W., Shenton, M.E., Ciszewski, A., Kasai, K., Lasko, N.B., Orr, S.P., Pitman, R.K., 2002. Smaller hippocampal volume predicts pathologic vulnerability to psychological trauma. Nat. Neurosci. 5, 1242–1247. https://doi.org/10.1038/nn958.

Golub, Y., Mauch, C.P., Dahlhoff, M., Wotjak, C.T., 2009. Consequences of extinction training on associative and non-associative fear in a mouse model of posttraumatic stress disorder (PTSD). Behav. Brain Res. 205, 544–549. https://doi.org/10.1016/j.bbr.2009.08.019.

Golub, Y., Kaltwasser, S.F., Mauch, C.P., Herrmann, L., Schmidt, U., Holsboer, F., Czisch, M., Wotjak, C.T., 2011. Reduced hippocampus volume in the mouse model of posttraumatic stress disorder. J. Psychiatr. Res. 45, 650–659. https://doi.org/10.1016/j.jpsychires.2010.10.014.

Gould, E., McEwen, B.S., Tanapat, P., Galea, L.A.M., Fuchs, E., 1997. Neurogenesis in the dentate gyrus of the adult tree shrew is regulated by psychosocial stress and NMDA receptor activation. J. Neurosci. 17, 2492–2498. https://doi.org/10.1523/jneurosci.17-07-02492.1997.

Grewal, S.S., Shepherd, J.K., Bill, D.J., Fletcher, A., Dourish, C.T., 1997. Behavioural and pharmacological characterisation of the canopy stretched attend posture test as a model of anxiety in mice and rats. Psychopharmacology 133, 29–38. https://doi.org/10.1007/s002130050367.

Heinz, D.E., Genewsky, A., Wotjak, C.T., 2017. Enhanced anandamide signaling reduces flight behavior elicited by an approaching robo-beetle. Neuropharmacology 126, 233–241. https://doi.org/10.1016/j.neuropharm.2017.09.010.

Herrmann, L., Ionescu, I.A., Henes, K., Golub, Y., Wang, N.X.R., Buell, D.R., Holsboer, F., Wotjak, C.T., Schmidt, U., 2012. Long-lasting hippocampal synaptic protein loss in a mouse model of posttraumatic stress disorder. PLoS One 7. https://doi.org/10.1371/journal.pone.0042603.

Hikishima, K., Komaki, Y., Seki, F., Ohnishi, Y., Okano, H.J., Okano, H., 2017. In vivo microscopic voxel-based morphometry with a brain template to characterize strainspecific structures in the mouse brain. Sci. Rep. 7, 1–9. https://doi.org/10.1038/s41598-017-00148-1.

Kao, C.Y., Stalla, G., Stalla, J., Wotjak, C.T., Anderzhanova, E., 2015. Norepinephrine and corticosterone in the medial prefrontal cortex and hippocampus predict PTSD-like symptoms in mice. Eur. J. Neurosci. 41, 1139–1148. https://doi.org/10.1111/ejn.12860.

Kassem, M.S., Lagopoulos, J., Stait-Gardner, T., Price, W.S., Chohan, T.W., Arnold, J.C., Hatton, S.N., Bennett, M.R., 2013. Stress-induced grey matter loss determined by MRI is primarily due to loss of dendrites and their synapses. Mol. Neurobiol. 47, 645–661. https://doi.org/10.1007/s12035-012-8365-7.

Kawakami, R., Shinohara, Y., Kato, Y., Sugiyama, H., Shigemoto, R., Ito, I., 2003. Asymmetrical allocation of NMDA receptor ε2 subunits in hippocampal circuitry. Science 300, 990–994. https://doi.org/10.1126/science.1082609.

Li, L., Wu, M., Liao, Y., Ouyang, L., Du, M., Lei, D., Chen, L., Yao, L., Huang, X., Gong, Q., 2014. Grey matter reduction associated with posttraumatic stress disorder and traumatic stress. Neurosci. Biobehav. Rev. 43, 163–172. https://doi.org/10.1016/j.neubiorev.2014.04.003.

Logue, M.W., van Rooij, S.J.H., Dennis, E.L., Davis, S.L., Hayes, J.P., Stevens, J.S., Densmore, M., Haswell, C.C., Ipser, J., Koch, S.B.J., Korgaonkar, M., Lebois, L.A.M., Peverill, M., Baker, J.T., Boedhoe, P.S.W., Frijling, J.L., Gruber, S.A., Harpaz-Rotem, I., Jahanshad, N., Koopowitz, S., Levy, I., Nawijn, L., O'Connor, L., Olff, M., Salat, D.H., Sheridan, M.A., Spielberg, J.M., van Zuiden, M., Winternitz, S.R., Wolff, J.D., Wolf, E.J., Wang, X., Wrocklage, K., Abdallah, C.G., Bryant, R.A., Geuze, E., Jovanovic, T., Kaufman, M.L., King, A.P., Krystal, J.H., Lagopoulos, J., Bennett, M., Lanius, R., Liberzon, I., McGlinchey, R.E., McLaughlin, K.A., Milberg, W.P., Miller, M.W., Ressler, K.J., Veltman, D.J., Stein, D.J., Thomaes, K., Thompson, P.M., Morey, R.A., 2018. Smaller hippocampal volume in posttraumatic stress disorder: a multisite ENIGMA-PGC study: subcortical volumetry results from posttraumatic stress disorder consortia. Biol. Psychiatry 83, 244–253. https://doi.org/10.1016/j.biopsych.2017.09.006.

Luo, Y., Liu, Y., Qin, Y., Zhang, X., Ma, T., Wu, W., Yang, Y., Jiang, D., Shan, H., Cao, Z., 2017. The atrophy and laterality of the hippocampal subfields in parents with or without posttraumatic stress disorder who lost their only child in China. Neurol. Sci. 38, 1241–1247. https://doi.org/10.1007/s10072-017-2952-3.

Lupien, S.J., De Leon, M., De Santi, S., Convit, A., Tarshish, C., Nair, N.P.V., Thakur, M., McEwen, B.S., Hauger, R.L., Meaney, M.J., 1998. Cortisol levels during human aging predict hippocampal atrophy and memory deficits. Nat. Neurosci. 1, 69–73. https://doi.org/10.1038/271.

Manjón, J.V., Coupé, P., Martí-Bonmatí, L., Collins, D.L., Robles, M., 2010. Adaptive non-local means denoising of MR images with spatially varying noise levels. J. Magn. Reson. Imaging 31, 192–203. https://doi.org/10.1002/jmri.22003.

Mason, J.W., Giller, E.L., Kosten, T.R., Ostroff, R.B., Podd, L., 1986. Urinary free-cortisol levels in posttraumatic stress disorder patients. J. Nerv. Ment. Dis. https://doi.org/10.1097/00005053-198603000-00003.

Meng, Y., Qiu, C., Zhu, H., Lama, S., Lui, S., Gong, Q., Zhang, W., 2014. Anatomical deficits in adult posttraumatic stress disorder: a meta-analysis of voxel-based morphometry studies. Behav. Brain Res. 270, 307–315. https://doi.org/10.1016/j.bbr.2014.05.021.

O'Doherty, D.C.M., Chitty, K.M., Saddiqui, S., Bennett, M.R., Lagopoulos, J., 2015. A systematic review and meta-analysis of magnetic resonance imaging measurement of structural volumes in posttraumatic stress disorder. Psychiatry Res. Neuroimaging 232, 1–33. https://doi.org/10.1016/j.pscychresns.2015.01.002.

Orr, S.P., Lasko, N.B., Shalev, A.Y., Pitman, R.K., 1995. Physiologic responses to loud tones in Vietnam Veterans with posttraumatic stress disorder. J. Abnorm. Psychol. 104, 75–82. https://doi.org/10.1037/0021-843X.104.1.75.

Pruessner, J.C., Baldwin, M.W., Dedovic, K., Renwick, R., Mahani, N.K., Lord, C., Meaney, M., Lupien, S., 2005. Self-esteem, locus of control, hippocampal volume, and cortisol regulation in young and old adulthood. Neuroimage 28, 815–826. https://doi.org/10.1016/j.neuroimage.2005.06.014.

Pulliam, J.V.K., Dawaghreh, A.M., Alema-Mensah, E., Plotsky, P.M., 2010. Social defeat stress produces prolonged alterations in acoustic startle and body weight gain in male long Evans rats. J. Psychiatr. Res. 44, 106–111. https://doi.org/10.1016/j.jpsychires.2009.05.005.

Radley, J.J., Rocher, A.B., Miller, M., Janssen, W.G.M., Liston, C., Hof, P.R., McEwen, B.S., Morrison, J.H., 2006. Repeated stress induces dendritic spine loss in the rat medial prefrontal cortex. Cereb. Cortex 16, 313–320. https://doi.org/10.1093/cercor/bhi104.

Shalev, A.Y., Rogel-Fuchs, Y., 1992. Auditory startle reflex in post-traumatic stress disorder patients treated with clonazepam. Isr. J. Psychiatry Relat. Sci. 29, 1–6.

Shin, L.M., Orr, S.P., Carson, M.A., Rauch, S.L., Macklin, M.L., Lasko, N.B., Peters, P.M., Metzger, L.J., Dougherty, D.D., Cannistraro, P.A., Alpert, N.M., Fischman, A.J., Pitman, R.K., 2004. Regional cerebral blood flow in the amygdala and medial prefrontal cortex during traumatic imagery in male and female Vietnam veterans with PTSD. Arch. Gen. Psychiatry 61, 168–176. https://doi.org/10.1001/archpsyc.61.2.168.

Shucard, J.L., Cox, J., Shucard, D.W., Fetter, H., Chung, C., Ramasamy, D., Violanti, J., 2012. Symptoms of posttraumatic stress disorder and exposure to traumatic stressors are related to brain structural volumes and behavioral measures of affective stimulus processing in police officers. Psychiatry Res. 204, 25–31. https://doi.org/10.1016/j.pscychresns.2012.04.006.

Siegmund, A., Wotjak, C.T., 2007. A mouse model of posttraumatic stress disorder that distinguishes between conditioned and sensitised fear. J. Psychiatr. Res. 41, 848–860. https://doi.org/10.1016/j.jpsychires.2006.07.017.

Steriade, M., 1996. Arousal: revisiting the reticular activating system. Science 272, 225–226. https://doi.org/10.1126/science.272.5259.225.

Sussman, D., Pang, E.W., Jetly, R., Dunkley, B.T., Taylor, M.J., 2016. Neuroanatomical features in soldiers with post-traumatic stress disorder. BMC Neurosci. 17, 1–11. https://doi.org/10.1186/s12868-016-0247-x.

Teicher, M.H., Anderson, C.M., Polcari, A., 2012. Childhood maltreatment is associated with reduced volume in the hippocampal subfields CA3, dentate gyrus,and subiculum. Proc. Natl. Acad. Sci. U. S. A. 109 https://doi.org/10.1073/pnas.1115396109.

Thome, J., Densmore, M., Koppe, G., Terpou, B., Théberge, J., McKinnon, M.C., Lanius, R.A., 2019. Back to the basics: resting state functional connectivity of the reticular activation system in PTSD and its dissociative subtype. Chronic Stress 3. https://doi.org/10.1177/2470547019873663, 247054701987366.

Verbitsky, A., Dopfel, D., Zhang, N., 2020. Rodent models of post-traumatic stress disorder: behavioral assessment. Transl. Psychiatry 10. https://doi.org/10.1038/s41398-020-0806-x.

Wang, Z., Neylan, T.C., Mueller, S.G., Lenoci, M., Truran, D., Marmar, C.R., Weiner, M.W., Schuff, N., 2010. Magnetic resonance imaging of hippocampal subfields in posttraumatic stress disorder. Arch. Gen. Psychiatry 67, 296–303. https://doi.org/10.1001/archgenpsychiatry.2009.205.

Wignall, E.L., Dickson, J.M., Vaughan, P., Farrow, T.F.D., Wilkinson, I.D., Hunter, M.D., Woodruff, P.W.R., 2004. Smaller hippocampal volume in patients with recent-onset posttraumatic stress disorder. Biol. Psychiatry 56, 832–836. https://doi.org/10.1016/j.biopsych.2004.09.015.

Woodward, S.H., Kaloupek, D.G., Streeter, C.C., Martinez, C., Schaer, M., Eliez, S., 2006. Decreased anterior cingulate volume in combat-related PTSD. Biol. Psychiatry 59, 582–587. https://doi.org/10.1016/j.biopsych.2005.07.033.

Woon, F.L., Sood, S., Hedges, D.W., 2010. Hippocampal volume deficits associated with exposure to psychological trauma and posttraumatic stress disorder in adults: a meta-analysis. Prog. Neuro-Psychopharmacol. Biol. Psychiatry 34, 1181–1188. https://doi.org/10.1016/j.pnpbp.2010.06.016.

Yamasue, H., Kasai, K., Iwanami, A., Ohtani, T., Yamada, H., Abe, O., Kuroki, N., Fukuda, R., Tochigi, M., Furukawa, S., Sadamatsu, M., Sasaki, T., Aoki, S., Ohtomo, K., Asukai, N., Kato, N., 2003. Voxel-based analysis of MRI reveals anterior cingulate gray-matter volume reduction in posttraumatic stress disorder due to terrorism. Proc. Natl. Acad. Sci. U. S. A. 100, 9039–9043. https://doi.org/10.1073/pnas.1530467100.

Yehuda, R., Teicher, M.H., Trestman, R.L., Levengood, R.A., Siever, L.J., 1996. Cortisol regulation in posttraumatic stress disorder and major depression: a chronobiological analysis. Biol. Psychiatry 40, 79–88. https://doi.org/10.1016/0006-3223(95)00451-3.

Yilmaz, M., Meister, M., 2013. Rapid innate defensive responses of mice to looming visual stimuli. Curr. Biol. 23, 2011–2015. https://doi.org/10.1016/j.cub.2013.08.015.